J. Phys. B: At. Mol. Opt. Phys. **33** (2000) 3713–3723. Printed in the UK PII: S0953-4075(00)50976-6

Electron-impact cross sections of Ne

S Tsurubuchi, K Arakawa, S Kinokuni and K Motohashi

Department of Applied Physics, Faculty of Technology, Tokyo University of Agriculture and Technology, Koganei-shi, Tokyo 184-8588, Japan

Received 5 June 2000, in final form 25 July 2000

Abstract. Electron-impact absolute emission cross sections were measured for the 3p → 3s transitions of Ne. Excitation functions of the 3s → 2p first resonance lines were measured in the energy range from the threshold to 1000 eV by a polarization-free optical method and relative cross sections were normalized to the absolute values, $(41.0 \pm 5.4) \times 10^{-19}$ cm^2 for the 73.6 nm line and $(7.1 \pm 1.0) \times 10^{-19}$ cm^2 for the 74.4 nm line, which were determined at 500 eV. The integrated level-excitation cross sections of Suzuki *et al* for the $1s_2$ and $1s_4$ levels were combined with the corresponding 3p → 3s cascade cross sections obtained in this paper to give absolute emission cross sections for the resonance lines. The level-excitation cross sections of the $1s_2$ and $1s_4$ states in Paschen notation were determined from the threshold to 1000 eV by subtracting 3p → 3s cascade cross sections from the corresponding 3s → 2p emission cross sections of the resonance lines. A large cascade contribution is found in the emission cross section of the resonance lines. It is 28.5% for the 73.6 nm line and 49.6% for the 74.4 nm line at 40 eV, and 17.0 and 61.8%, respectively, at 300 eV.

1. Introduction

Electron-impact emission cross sections of the Ne atom are of importance not only in the field of fundamental physics but also for the further understanding of discharge plasmas such as in laser systems and of atomic processes in astrophysics. A related level diagram is presented in figure 1. Because *LS* coupling does not hold for Ne, Paschen notation is used for level assignment; the corresponding Racah notation is given in table 1 (Moor 1971).

So far, a few experiments have been reported in the visible wavelength range (Feltsan *et al* 1966, Herrmann 1936, Hanle 1930). Sharpton *et al* (1970) carried out a systematic measurement for the 3p → 3s transitions. Emission cross sections for the 73.6 nm and 74.4 nm resonance lines were given by Hertz (1969) and by Kanik *et al* (1996) for VUV measurements. The emission cross section for the $1s_2$ → 2p resonance line was measured by de Jongh (1971) and relative excitation functions by van Raan (1973). Tan *et al* (1974) measured emission cross sections for the 73.6 nm resonance line from 100–1000 eV. A survey is presented by Heddle and Gallagher (1989).

Register *et al* (1984) measured the differential excitation cross sections of the $1s_2$–$1s_5$ levels from 10° to 140° by an energy-loss measurement and gave the integrated excitation cross sections for those levels at 25, 30, 50 and 100 eV. Suzuki *et al* (1994) presented the differential cross sections and generalized oscillator strengths for the $1s_2$, $1s_4$ and $2p_1$ levels by an electron-impact energy-loss measurement and gave integrated level-excitation cross sections for the $1s_2$ and $1s_4$ levels at 300, 400 and 500 eV. Miers *et al* (1982) and Philips *et al* (1985) measured integrated cross sections for the excitation of the $1s_2$–$1s_5$ levels by laser excitation fluorescence techniques. In this paper, the absolute cross sections for the 3p → 3s

0953-4075/00/183713+11$30.00

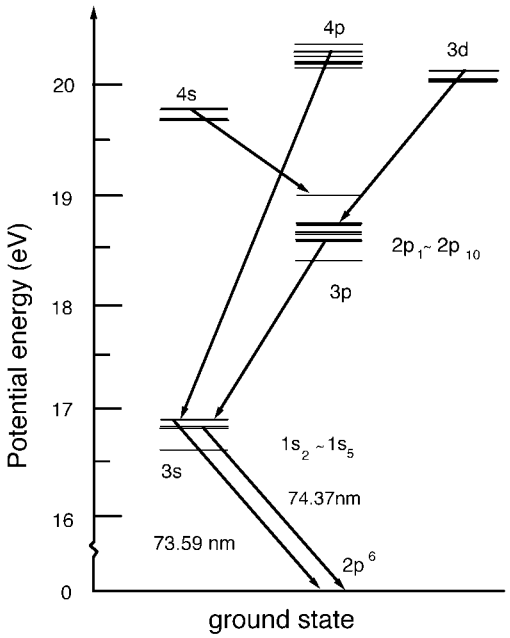

Figure 1. Energy level diagram of Ne.

transitions and relative excitation functions for the 3s → 2p resonance lines were measured in the energy range from threshold to 1000 eV by a polarization-free optical measurement. The level-excitation cross sections of the $1s_2$ and $1s_4$ states were determined by subtracting 3p → 3s cascade cross sections from the corresponding 3s → 2p emission cross sections of the resonance lines over the wide range of impact energies. Zeman and Bartschat (1997) performed a 31-state semirelativistic Breit–Pauli *R*-matrix calculation. Machado *et al* (1984) presented integrated excitation cross sections as well as differential cross sections with the first-order many-body theory (FOMBT). Their results are compared with the experimental ones.

2. Experimental procedure

An electron gun with a barium oxide cathode was oriented so as to make polarization-free measurements possible, i.e. it was set at the double magic angle. The outline of the experimental apparatus and procedures used is essentially the same as described before (Tsurubuchi *et al* 1996). A monochromator with a photomultiplier was used for the visible wavelength range and a Seya-Namioka vacuum monochromator was used for intensity measurements in the VUV region. The diameter of the Rowland circle of the VUV monochromator is 498.1 mm. A Cu–BeO plate coated with caesium iodide was used as a photocathode to enhance the detection efficiency of a channel electron multiplier.

The electron beam was modulated for a synchronous single photon-counting measurement. The target gas was introduced continuously into the chamber through a needle valve and the pressure inside was measured by an ionization gauge calibrated with a capacitance manometer. The absolute cross section for the 3p → 3s transitions was obtained by comparing line intensities with that of the Ar 750.3 nm line, whose emission cross section was obtained by an absolute measurement of the line intensity (Tsurubuchi *et al* 1996).

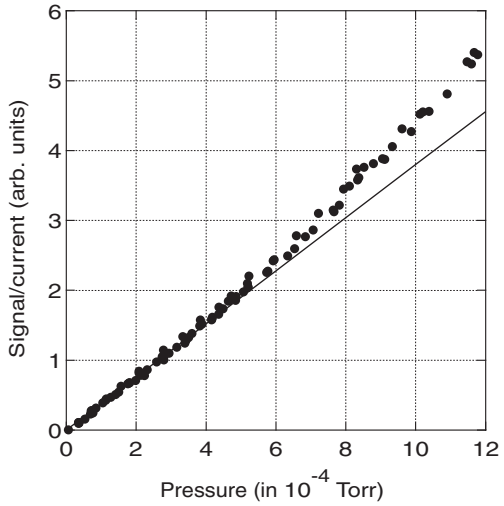

Figure 2. Pressure dependence of emitted intensities of the $2p_8 \rightarrow 1s_4$ (650.65 nm) line.

In the visible wavelength range, the overall sensitivity of the detection system was determined by use of a standard light source of moderate intensity for a counting measurement, and its emission intensity was calibrated by comparing the brightness with that of an calibrated EPUV tungsten-strip lamp operated at an alternating current of 35 A. The wavelength range covered with the working standard source is 400–750 nm. Above 750 nm, the branching ratio method was used for Ar lines with the transition probabilities summarized by Wiese *et al* (1969, 1989). The line pairs used are $2p_2 \rightarrow 1s_5$ (696.5 nm) and $2p_2 \rightarrow 1s_2$ (826.4 nm); $2p_3 \rightarrow 1s_4$ (738.4 nm) and $2p_3 \rightarrow 1s_2$ (840.8 nm); $2p_4 \rightarrow 1s_5$ (714.7 nm) and $2p_4 \rightarrow 1s_3$ (794.8 nm); $2p_4 \rightarrow 1s_3$ (794.8 nm) and $2p_4 \rightarrow 1s_2$ (852.1 nm); $2p_6 \rightarrow 1s_5$ (763.5 nm) and $2p_6 \rightarrow 1s_4$ (800.6 nm); and $2p_8 \rightarrow 1s_5$ (801.5 nm) and $2p_8 \rightarrow 1s_4$ (842.4 nm).

Figure 2 shows the pressure dependence of the 650.65 nm line ($2p_8 \rightarrow 1s_4$) intensity at 100 eV. The signal intensity starts to deviate from a straight line above 6×10^{-4} Torr. Therefore, the present measurements for the 3p, 4p $\rightarrow$ 3s group were carried out at a target pressure below 5×10^{-4} Torr. In the case of the resonance lines, the target pressure was kept as low as 5.5×10^{-6} Torr during measurements to reduce the possible effect of radiation trapping.

The steady-state population of the $1s_2$ and $1s_4$ states is determined by the 3p, 4p $\rightarrow$ 3s cascading transitions to those states, in addition to the direct level-excitation processes. The 3p $\rightarrow$ 3s emission lines of the cascading transitions to the $1s_2$ and $1s_4$ states are all in the visible range and cross sections can be measured with considerable accuracy, while the level-excitation cross sections for those states are presented by an electron-energy-loss measurement at 300, 400 and 500 eV (Suzuki *et al* 1994). The 3s $\rightarrow$ 2p emission cross section is given by $Q_{3s\rightarrow 2p} = Q_{3s} + \sum Q_{nl\rightarrow 3s}$ ($n \geqslant 3$) where Q_{3s} is the level-excitation cross section and $\sum Q_{nl\rightarrow 3s}$ is the sum of the cascading cross section to the 3s level from the upper states, which is mostly composed of the 3p $\rightarrow$ 3s transitions. It is, therefore, possible to determine an absolute emission cross section for the resonance line by a combination of those data without measuring the absolute sensitivity of the detection system in the VUV region. The polarization-free relative excitation functions of the resonance lines were measured at constant target pressure in the energy range from threshold to 1000 eV and were normalized to the absolute emission cross sections determined at 500 eV. The level-excitation cross sections for

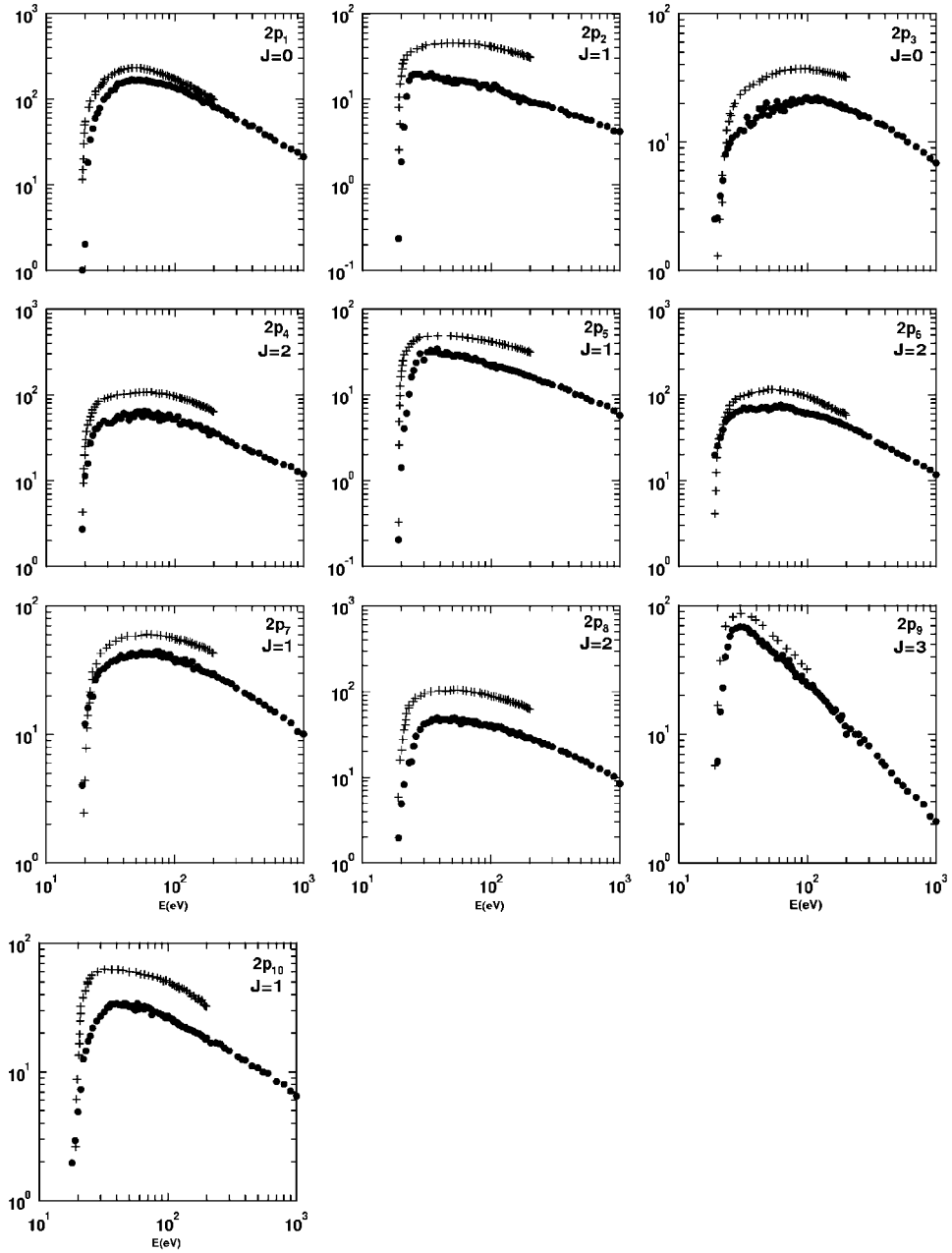

Figure 3. Apparent cross sections for the 3p → 3s transitions of Ne in units of 10^{-20} cm^2. Present result (●); Sharpton *et al* (1970) (+).

the $1s_2$ and $1s_4$ states are, in turn, obtained over a wide range of impact energies by subtracting the 3p → 3s cascade cross sections from the corresponding 3s → 2p emission cross sections of the resonance lines. The process of determining the absolute scale of the level-excitation cross section was essentially the same as the normalization to the data of Suzuki *et al* (1994) at 500 eV.

Table 1. $3p \rightarrow 3s$ emission cross sections and apparent excitation cross sections, Q_i^a, of the 3p state of Ne ($\times 10^{-20}$ cm^2 at 100 eV). The top line of each group represents the wavelength (Striganov and Sventitskii 1968) in nm. Both Paschen and Racah notations are given for each level (Moor 1971).

	$1s_2$ $3s'[\frac{1}{2}]_1^o$	$1s_3$ $3s'[\frac{1}{2}]_0^o$	$1s_4$ $3s[\frac{3}{2}]_1^o$	$1s_5$ $3s[\frac{3}{2}]_2^o$	Q_i^a
$2p_1$	585.24 nm	—	540.05	—	
$3p'[\frac{1}{2}]_0$	135 ± 19		1.8 ± 0.3[a]		137 ± 19
$2p_2$	659.89	616.35	602.99	588.18	
$3p'[\frac{1}{2}]_1$	5.6 ± 0.8	3.5 ± 0.5	1.4 ± 0.2[a]	2.8 ± 0.4	13.3 ± 1.9
$2p_3$	665.20	—	607.43	—	
$3p[\frac{1}{2}]_0$	0.11 ± 0.02[a]		22.0 ± 3.1		22.1 ± 3.1
$2p_4$	667.82	—	609.61	594.48	
$3p'[\frac{3}{2}]_2$	23.0 ± 3.2		17.8 ± 2.5	11.2 ± 1.6[a]	52.0 ± 7.3
$2p_5$	671.70	626.64	612.84	597.55	
$3p'[\frac{3}{2}]_1$	9.3 ± 1.3	10.7 ± 1.5	0.29 ± 0.04[a]	1.5 ± 0.2[a]	21.8 ± 3.0
$2p_6$	692.94	—	630.47	614.30	
$3p[\frac{3}{2}]_2$	21.5 ± 4.6		5.2 ± 0.7[a]	34.8 ± 4.9[a]	62 ± 10
$2p_7$	702.40	653.28	638.29	621.72	
$3p[\frac{3}{2}]_1$	1.4 ± 0.2[a]	7.7 ± 1.1	23.0 ± 3.2	4.6 ± 0.6	36.7 ± 5.1
$2p_8$	717.39	—	650.65	633.44	
$3p[\frac{5}{2}]_2$	2.4 ± 0.3[a]		24.8 ± 5.3	13.3 ± 1.9	40.5 ± 5.7
$2p_9$	—	—	—	640.22	
$3p[\frac{5}{2}]_3$				24.0 ± 3.4	24.0 ± 3.4
$2p_{10}$	808.24	743.88	724.51	703.24	
$3p[\frac{1}{2}]_1$	0.08 ± 0.01[a]	1.7 ± 0.2[a]	6.9 ± 0.9	18.7 ± 2.6	27.4 ± 3.7
Total	198 ± 29	23.6 ± 3.3	103 ± 14	111 ± 16	436 ± 62

[a] Cross sections were derived by use of the transition probabilities given by Wiese and Martin (1980).

3. Results and discussion

3.1. $3p \rightarrow 3s$ emission cross sections

Figure 3 shows the present results of the apparent excitation cross section, Q_i^a, of the $2p_1$ to $2p_{10}$ states, i.e. excitation cross sections of those levels including cascade transitions ($Q_i^a = \sum_j Q_{2p_i \rightarrow 1s_j}$, $i = 1$–10). The numerical values at 100 eV are listed in table 1. Excitation functions with the same J show similar energy dependences. Although it can be considered as a reflection of the characteristics of excited 3p states, we have to take into account the fact that the cascading contribution from the $nl \rightarrow 3p$ transitions is involved in the $3p \rightarrow 3s$ cross section. It is well known that the $2p_9$ level is a pure triplet state, $^3D_3$ in the LS scheme, but the experimentally obtained energy dependence of the $2p_9 \rightarrow 1s_5$ (640.2 nm) line emission cross section, for example, is $\propto E^{-1}$ and not $\propto E^{-3}$ (Ochkur 1964) at high energies, where E is the energy of impact electrons.

It is worthwhile noticing that the emission cross sections of the cascading transitions, $4d \rightarrow 2p_9$ (576.4 nm) and $5d \rightarrow 2p_9$ (503.7 nm), for example, show a very similar energy dependence at high energies to the $2p_9 \rightarrow 1s_5$ cross section, as shown in figure 4. This fact indicates that the cascading contribution accounts for most of the population of the $2p_9$

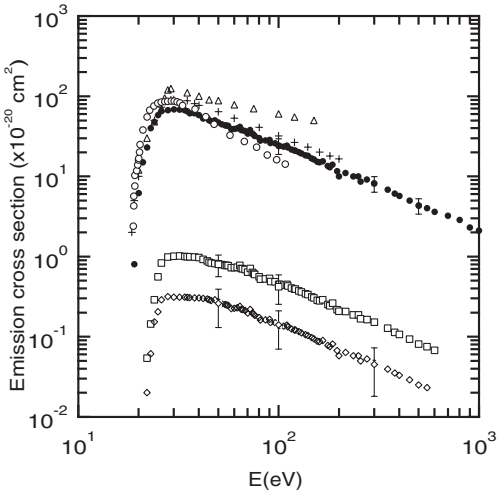

Figure 4. Excitation function of the $2p_9 \rightarrow 1s_5$ (640.2 nm) line of Ne. Present result (●); Sharpton *et al* (1970) (+), Gay *et al* (1996) (○), Feltsan *et al* (1966) (△), emission cross sections of the 576.4 nm (□) and 503.7 nm (◇) lines.

level. This kind of situation will probably be the case for the high-energy behaviour of the $2p_9 \rightarrow 1s_5$, $(4p[5/2]_3 \rightarrow 4s[3/2]_2)$ transition of Ar (Chilton 1998). The energy dependence of the $3p \rightarrow 3s$ group of Feltsan *et al* (1966) shows a slower decrease at high energies, while the result of Gay *et al* (1996) seems to fall off more rapidly.

Sharpton *et al* (1970) carried out a systematic measurement of cross sections in the visible spectral range from the threshold to 200 eV. It seems that their absolute values are systematically too large compared with ours, probably due to their using too high a target pressure ($<3 \times 10^{-2}$ Torr). In the case of Feltsan *et al* (1966), the target pressure used was $(0.7–3) \times 10^{-3}$ Torr. A careful examination of line intensity against target pressure reveals that the $3p \rightarrow 3s$ signal intensity starts to deviate from a straight line above 5.5×10^{-4} Torr, as stated before. This fact tells us why their cross sections showed larger values than the present ones. The secondary processes play a role at high target pressure in line intensity measurements. In this paper, the measurements for the 3p, $4p \rightarrow 3s$ group, therefore, were carried out at a target pressure below 5×10^{-4} Torr.

The total $3p \rightarrow 3s$ cascade cross section in populating the $1s_2$ state is $(198 \pm 29) \times 10^{-20}$ cm^2 at 100 eV, and $(23.6 \pm 3.3) \times 10^{-20}$, $(103 \pm 14) \times 10^{-20}$, $(111 \pm 16) \times 10^{-20}$ cm^2 for the $1s_3$, $1s_4$ and $1s_5$ states, respectively. The total cross section of the $3p \rightarrow 3s$ transition is estimated as $(436 \pm 62) \times 10^{-20}$ cm^2 at 100 eV. Figure 5 illustrates the energy dependence of the total cascading cross sections to the $1s_2$, $1s_3$, $1s_4$ and $1s_5$ states.

3.2. Emission cross sections of the resonance lines

In the case of VUV measurement, the target pressure was kept as low as 5.5×10^{-6} Torr in order to reduce possible effects due to radiation trapping. Transmission curves of emitted resonance radiation of rare gases were investigated in detail for the present optical system by Tsurubuchi *et al* (1990). In table 2 the normalization step of the relative excitation functions of the resonance lines is given. In this estimation, only the $3p \rightarrow 3s$ transitions are taken into account because the line intensities of the $4p \rightarrow 3s$ group are considerably weaker compared

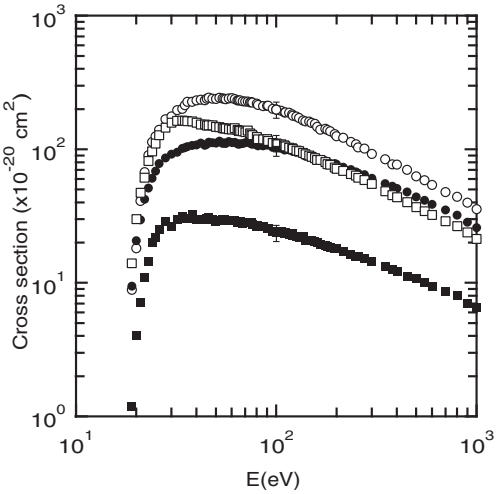

Figure 5. The total cascade cross sections populating the $1s_2$ (○), $1s_4$ (●) resonant states and the $1s_5$ (□) and $1s_3$ (■) metastable states.

Table 2. Emission cross sections of the 3s→2p resonance lines ($\times 10^{-19}$ cm^2 at 500 eV).

	3s levels	
	$1s_2$, $3s'[\frac{1}{2}]_1^o$	$1s_4$, $3s[\frac{3}{2}]_1^o$
Sum of the 3p → 3s emission cross sections	6.3 ± 0.9	4.4 ± 0.6
Level-excitation cross section (Suzuki *et al* 1994)	34.7 ± 4.5	2.72 ± 0.35
Emission cross sections of the 3s → 2p resonance lines	41.0 ± 5.4	7.1 ± 1.0

with those of the 3p → 3s group. The most prominent line in the 4p → 3s group is the 352.0 nm line ($3p_1 \rightarrow 1s_2$) and its emission cross section obtained in this paper is $(7.2 \pm 1.5) \times 10^{-20}$ cm^2 at 100 eV.

Emission cross sections of the resonance lines are given in figures 6 and 7. Numerical values are listed in table 3. The cross section of Kanik *et al* (1996) for the 73.6 nm line shows complete overlap with the present data over the whole range of impact energies. For the 74.4 nm lines, the present result is in agreement with their result, to within estimated errors. The results of de Jong (1971) and Tan *et al* (1974) for the 73.6 nm line all show good agreement, to within estimated errors. The cross section of Hertz (1969) seems too large. The result of the LIF method of Philips *et al* (1985) for the 73.6 nm line shows a slightly different energy dependence at low energies. For the 74.4 nm line, the values of Hertz (1969) and Philips *et al* (1985) show larger values than the present ones at high energies.

A large cascade contribution was found in the emission cross section of the resonance line (Miers *et al* 1982). We have found that the percentage cascade contribution to the resonance lines is 28.5% for the 73.6 nm line and 49.6% for the 74.4 nm line at 40 eV, and 17.0 and 61.8%, respectively, at 300 eV. The uncertainty of 14.3% is included in the summed absolute values of the visible cross sections. Neglect of 4p, 5p → 3s transitions in the estimation of the cascading contribution introduces about 5% of error. The level-excitation cross section of Suzuki *et al* (1994) is determined to within 13%. The reproducibility of the excitation function is within 3%. The uncertainty in the absolute value of cross sections of the resonance lines is finally estimated to be 20.2%.

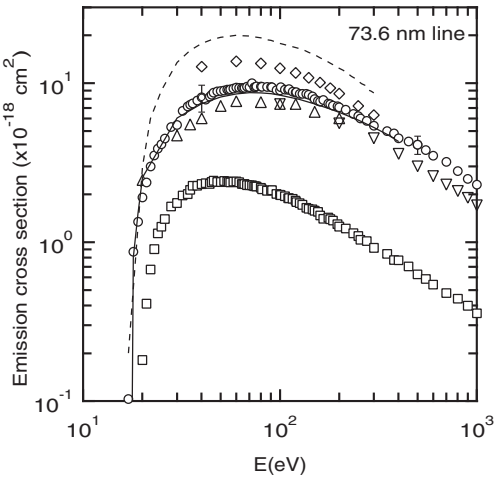

Figure 6. Emission cross sections of the 73.6 nm line of Ne. Present result (○), de Jongh (1971) (△), Hertz (1969) (- - - -), Tan *et al* (1974) (▽), Philips *et al* (1985) (◇), Kanik *et al* (1996) (——), total cascade to the $1s_2$ level (□).

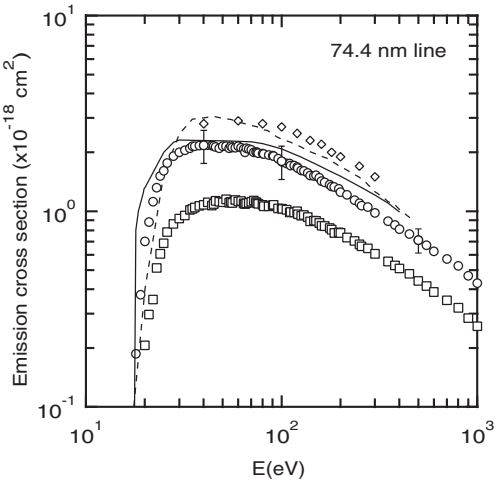

Figure 7. Emission cross sections of the 74.4 nm line of Ne. Present result (○), Philips *et al* (1985) (◇), Kanik *et al* (1996) (——), Hertz (1969) (- - - -), total cascade to the $1s_4$ level (□).

3.3. Level-excitation cross section

The level-excitation cross sections of the $1s_2$ and $1s_4$ states can be obtained if the cascade cross sections for these states are subtracted from the corresponding emission cross sections of the resonance lines. The results obtained are shown in figures 8 and 9. The numerical values are given in table 4. The values of de Jongh (1971) coincide with the present result, to within experimental errors. The excitation cross sections of Register *et al* (1984) for the $1s_2$ state show a slight deviation from ours at low energies. The difference between Philips *et al* (1985) and the present measurements seems to reflect the difference observed in the 73.6 nm line emission cross section, while excellent agreement is observed for the level-excitation cross

Table 3. Emission cross sections of the resonance lines ($\times 10^{-18}$ cm^2).

Energy (eV)	73.59 nm	74.37 nm
18	0.87	0.19
20	1.91	0.70
30	5.46	1.97
40	8.15	2.20
50	8.91	2.15
60	9.38	2.12
70	9.44	2.01
80	9.52	2.01
90	9.45	1.92
100	9.00	1.80
120	8.73	1.68
140	8.46	1.52
150	7.94	1.53
160	7.64	1.43
180	7.38	1.34
200	7.05	1.25
250	6.20	1.10
300	5.43	0.98
350	5.02	0.89
400	4.50	0.81
450	4.31	0.77
500	4.10	0.71
550	3.83	0.67
600	3.51	0.62
700	3.20	0.57
800	2.81	0.53
900	2.50	0.47
1000	2.30	0.43

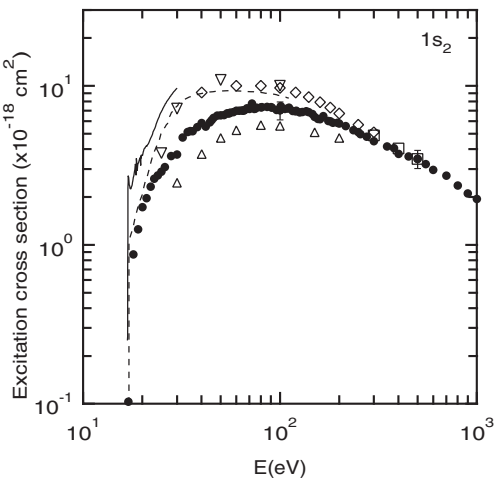

Figure 8. Level-excitation cross sections of the $1s_2$ state. Present result (●), Philips *et al* (1985) (◇), Register *et al* (1984) (▽), Suzuki *et al* (1994) (□), de Jongh (1971) (△) (see Register *et al* (1984)), Machado *et al* (1984) (- - - -), Zeman and Bartschat (1997) (——).

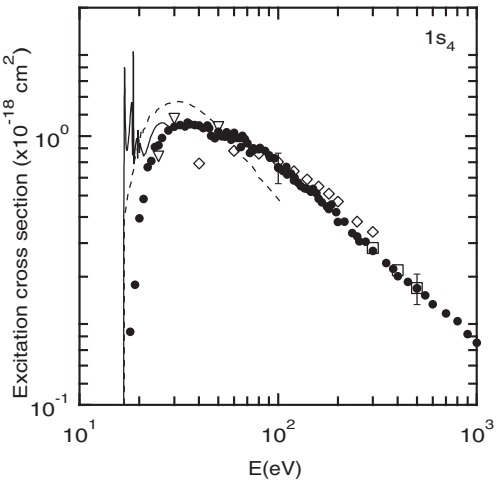

Figure 9. Level-excitation cross sections of the $1s_4$ state. Present result (●), Philips *et al* (1985) (◇), Register *et al* (1984) (▽), Suzuki *et al* (1994) (□), Machado *et al* (1984) (- - - -), Zeman and Bartschat (1997) (——).

Table 4. Level-excitation cross sections of the $1s_2$ and $1s_4$ levels ($\times 10^{-18}$ cm^2).

Energy (eV)	$1s_2$	$1s_4$
20	1.72	0.49
25	2.83	0.92
30	3.70	1.08
40	5.83	1.09
50	6.52	1.04
60	7.00	1.00
70	7.16	0.94
80	7.33	0.89
90	7.34	0.85
100	7.02	0.76
110	7.19	0.73
120	6.91	0.68
150	6.37	0.60
200	5.80	0.48
250	5.11	0.42
300	4.48	0.37
400	3.73	0.30
500	3.47	0.27
600	2.96	0.24
700	2.72	0.22
800	2.36	0.20
900	2.10	0.18
1000	1.94	0.17

section of the $1s_4$ state. The results for the $1s_4$ state show a fairly good agreement with the others. The energy resolution of the present setup was not enough to resolve the fine structures predicted by Zeman and Bartschat (1997) above threshold. A theoretical FOMBT result of Machado *et al* (1984) seems to have a more pronounced maximum at low energies, both for the $1s_2$ and $1s_4$ states, and shows a more rapid descent at high energies in the case of $1s_4$.

According to the Bethe theory, the excitation cross section at high energies is given by

$$\sigma_n = \frac{4\pi a_0^2 R}{E} \frac{R}{E_n} f_n \ln \frac{c_n E}{R}$$

where n represent the excited state, a_0 is the Bohr radius, R is the Rydberg constant, E is the impact energy, f_n is the optical oscillator strength and c_n is a constant (Inokuti 1971). By using the least-squares method above 200 eV, we have $f_n = 0.137 \pm 0.006$ with $c_n = 0.613$ for the $1s_2$ state and $f_n = 0.012 \pm 0.001$ with $c_n = 0.526$ for the $1s_4$ state, respectively, which can be compared with the previous work (Tsurubuchi *et al* 1990, Chan *et al* 1992). Agreement seems fairly good.

Acknowledgments

The authors would like to thank M Hyodoh and H Kobayashi for obtaining some of the data. This work has been partly supported by Grant-in-aid for Scientific Research (B) from the Japan Society for the Promotion of Science.

References

Chan W F, Cooper G, Guo X and Brion C E 1992 *Phys. Rev.* A **45** 1420
Chilton J E, Boffard J B, Schappe R S and Lin C C 1998 *Phys. Rev.* A **57** 267
de Jongh J P 1971 *PhD Thesis* University of Utrecht
Feltsan P V, Zapesochnyi I P and Povch M M 1966 *Ukr. Fiz. Zh.* **11** 1222
Gay T J, Furst J E, Trantham K W and Wijayaratna W M K P 1996 *Phys. Rev.* A **53** 1623
Hanle W 1930 *Z. Phys.* **65** 512
Heddle D W O and Gallagher J W 1989 *Rev. Mod. Phys.* **61** 221
Herrmann O 1936 *Ann. Phys., Lpz.* **25** 143
Hertz H 1969 *Z. Naturf.* **24A** 1937
Inokuti M 1971 *Rev. Mod. Phys.* **43** 297
Kanik I, Ajello J M and James G K 1996 *J. Phys. B: At. Mol. Opt. Phys.* **29** 2355
Machado L E, Lwal E P and Csanak G 1984 *Phys. Rev.* A **29** 1811
Miers R E, Gastineau J E, Philips M H, Anderson L W and Lin C C 1982 *Phys. Rev.* A **25** 1185
Moor C E 1971 *Atomic Energy Levels* NSRDS-NBS Circular no 35, vol 1 (Washington, DC: National Bureau of Standards)
Ochkur V I 1964 *Sov. Phys.–JETP* **18** 503
Philips M H, Anderson L W and Lin C C 1985 *Phys. Rev.* A **32** 2117
Register D F, Trajmar S, Steffensen G and Cartwright D C 1984 *Phys. Rev.* A **29** 1793
Sharpton F A, St John R M, Lin C C and Fajen F E 1970 *Phys. Rev.* A **2** 1305
Striganov A R and Sventitskii N S 1968 *Tables of Spectral Lines of Neutral and Ionized Atoms* (New York: Plenum)
Suzuki T Y, Suzuki H, Ohtani S, Min B S, Takayanagi T and Wakiya K 1994 *Phys. Rev.* A **49** 4578
Tan K-H, Donaldson F G and McConkey J W 1974 *Can. J. Phys.* **52** 786
Tsurubuchi S, Miyazaki T and Motohashi K 1996 *J. Phys. B: At. Mol. Opt. Phys.* **29** 1785
Tsurubuchi S, Watanabe K and Arikawa T 1990 *J. Phys. Soc. Japan* **59** 497
van Raan A F J 1973 *Physica* **65** 566
Wiese W L, Brault J M, Danzmann K, Helbig V and Kock M 1989 *Phys. Rev.* A **39** 2461
Wiese W L, Bridges J M, Kornblith R L and Kelleher D E 1969 *J. Opt. Soc. Am.* **59** 1206
Wiese W L and Martin G A 1980 *Wavelength and Transition Probabilities for Atoms and Atomic Ions* NSRDS-NBS Circular no 68, part II (Washington, DC: National Bureau of Standards)
Zeman V and Bartschat V 1997 *J. Phys. B: At. Mol. Opt. Phys.* **30** 4609